POLITECNICO DI TORINO
Repository ISTITUZIONALE

Effect of superabsorbent polymer introduction on properties of alkali-activated slag mortar

Original
Effect of superabsorbent polymer introduction on properties of alkali-activated slag mortar / Yang, Z., Shi, P., Zhang, Y., Li, Z.. - In: CONSTRUCTION AND BUILDING MATERIALS. - ISSN 0950-0618. - ELETTRONICO. - 340:(2022), p. 127541. [10.1016/j.conbuildmat.2022.127541]

Availability:
This version is available at: 11583/2969270 since: 2022-07-02T17:58:03Z

Publisher:
Elsevier

Published
DOI:10.1016/j.conbuildmat.2022.127541

Terms of use:

This article is made available under terms and conditions as specified in the corresponding bibliographic description in the repository

Publisher copyright

(Article begins on next page)

27 November 2026

Construction and Building Materials 340 (2022) 127541

Contents lists available at ScienceDirect

Construction and Building Materials

journal homepage: www.elsevier.com/locate/conbuildmat

Effect of superabsorbent polymer introduction on properties of alkali-activated slag mortar

Zhengxian Yang [a,1], Peng Shi [a,b,1], Yong Zhang [a], Zhenming Li [c,*]

[a] College of Civil Engineering, Research Center for Advanced Civil Engineering Materials, Fuzhou University, Fuzhou 350108, China
[b] Department of Structural, Geotechnical and Building Engineering, Politecnico di Torino, Turin 10129 Italy
[c] Department of Materials and Environment (Microlab), Faculty of Civil Engineering and Geoscience, Delft University of Technology, Delft, the Netherlands

ARTICLE INFO

Keywords:
Alkali activated slag
Superabsorbent polymer
Autogenous shrinkage
Strength
Permeability
Frost resistance

ABSTRACT

Internal curing by superabsorbent polymer (SAP) has been applied in alkali-activated slag (AAS) systems by a few previous studies with the purpose to mitigate the autogenous shrinkage. However, the effects of SAP on other properties of AAS have been rarely studied. In this paper, the workability, strength, permeability, and frost resistance of AAS mortar with synthesized SAP are investigated besides the autogenous shrinkage. Two SAP introducing ways (dry mixing and wet mixing) are considered. It is found that the flowability of AAS mortar decreases with the increase of SAP dosage regardless of the introducing way. The strength and permeability increase with the SAP dosage when it is below a certain amount depending on the mixing way. The autogenous shrinkage can be mitigated significantly by the incorporation of SAP and the mitigating effect is more pronounced by wet mixing. The frost resistance becomes better when more SAP is introduced in either way. The mechanisms behind these phenomena are explained based on the characterization results on the reaction kinetics, reaction products and pore structure of the mixtures with SAP.

1. Introduction

Concrete structures are widely used in various fields nowadays because of their high performance and low cost [1]. Ordinary Portland cement (OPC) is the primary raw material for the development of concrete industry [2]. The production process of cement normally involves grinding and burning of raw materials, which emit a large amount of pollutants such as CO_2, SO_2, NO_x, and dust [3–5]. In order to reduce the carbon footprint of the construction sector, various environmentally friendly alternatives to OPC have been developed. Alkali-activated slag (AAS) is one of such materials owing to its green features and satisfactory mechanical properties [4,6–10]. However, compared with OPC with or without supplementary materials, AAS is found to show much larger shrinkage [11–13], which can lead to cracking and seriously impair the durability of AAS based concrete structures [14].

For cementitious materials, many strategies have been identified to reduce the autogenous shrinkage and associated cracking tendency, among which internal curing has been proved as an effective one [15,16]. Compared to external curing which has effect mainly on the concrete surface, internal curing provides moisture from inside and can maintain a high internal relative humidity homogenously [17,18]. To provide internal curing, lightweight aggregate such as recycled aggregate, ceramsite, cuttlebone powder, and superabsorbent polymer (SAP) can be used [19–24]. SAP is normally made of high molecular structure materials which are rich in strong hydrophilic groups. Compared to lightweight aggregate, SAP has higher water absorption and better moisture retention capacity. Also, the release of water from SAP is more complete so that the internal curing effect is more remarkable.

Inspired by the promising effects of SAP identified in OPC systems [25,26], researchers have conducted several studies applying SAP in AAS. For example, Song et al. [27] reported that internal curing by SAP could reduce the autogenous shrinkage of AAS mortar. Tu et al. [23] found both the chemical shrinkage and autogenous shrinkage of alkali-activated slag-fly ash pastes can be reduced by SAP. Vafaei [28] observed not only reduced shrinkage but even expansion of SAP-incorporating AAS paste. Li et al. [29] monitored the internal curing process in AAS with SAP by X-ray micro-tomography and reported that the internal curing is also helpful to mitigate the cracking potential of restrained AAS. Irrespective of the different mixtures used in these studies, a consensus is that the autogenous shrinkage of alkali-activated

* Corresponding author.
E-mail address: z.li-2@tudelft.nl (Z. Li).
[1] They are co-first authors.

https://doi.org/10.1016/j.conbuildmat.2022.127541
Received 10 August 2021; Received in revised form 24 March 2022; Accepted 14 April 2022
Available online 8 May 2022
0950-0618/© 2022 The Author(s). Published by Elsevier Ltd. This is an open access article under the CC BY license (http://creativecommons.org/licenses/by/4.0/).

materials can be mitigated by internal curing with SAP.

However, it should be noted that the incorporation of SAP can influence various performances of concrete besides autogenous shrinkage. Mechtcherine [30] and Schröfl [31] found that the incorporation of SAP could outstandingly affect the yield stress and plastic viscosity of concrete. Snoeck et al. [32,33] indicated that SAP introduces additional water which leads to further hydration and self-healing of the cement matrix. Schröfl et al. [34] and Jensen and Hansen [35] reported that SAP added to cementitious materials can produce voids in the slurry which may have negative impacts on the strength. Differently, Mahta [36] considered that SAP can promote hydration and increase the strength. Möning [37] reported that the addition of SAP would introduce extra water to increase the gas content in the slurry so that the frost resistance of concrete could be improved [31,38]. Hasholt and Jensen [39] showed that the addition of SAP resulted in an increased gel porosity and a more tortuous pore structure, by which the chloride transport coefficient is reduced. These studies show that the incorporation of SAP has effects on not only shrinkage but also the reaction kinetics, pore structure, workability, and durability of cement. However, these effects of SAP on AAS systems have seldom been considered.

Besides the unclear multiple effects of SAP on AAS, disagreement exists on the introducing way of SAP. For example, Vafaei et al. [28] and Li et al. [29] mixed SAP with dry precursors first before the liquid was added. The only difference in these two studies was that Vafaei used higher water/binder ratios for mixtures with SAP while Li et al. applied additional alkali solution, i.e., higher activator/binder ratios. Although these researchers measured the absorption of SAP in solution by tea-bag method, the actual absorption of SAP pre-mixed with the precursors may not be the same. When liquid is added into the solids, SAP and precursor will compete in absorbing liquid. Moreover, the paste or mortar is normally with a certain viscosity so that the SAP particles cannot expand freely like in solution. Tu et al. [23] added half the solution first to mix with the precursor and another half with SAP, in which way, SAP may be able to absorb more liquid and to provide longer term of internal curing. However, no conclusion on mixing sequence can be drawn by comparing the results of these studies due to the different SAPs and mixtures used by the authors. The influence of introducing way of SAP on the properties of AAS systems remains unclear.

In this study, therefore, a self-synthesized SAP is used and investigation is conducted on the effects of SAP on different properties of AAS. The workability, strength, autogenous shrinkage, permeability, and frost resistance of AAS mortar with and without SAP are comprehensively studied. The influences of dry mixing and wet mixing of SAP on the properties of AAS are compared. Based on the microstructural characterization results, the role of SAP in fresh and hardened AAS is discussed.

2. Materials and testing methods

2.1. Raw materials

Slag, standard sands, polycarboxylate superplasticizer, and SAP were used in this paper. The S95 grade slag was from Shanxi Longze Water Purification Material Co., Ltd, with a specific surface area of 1310 m^2/kg and a density of 2.91 g/cm^3. The chemical composition of slag is shown in Table 1. The X-ray diffraction (XRD) pattern of the slag is shown in Fig. 1 (a). It can be seen that the slag contained mainly amorphous phases and a small amount of quartz and calcite.

The SAP was a three-dimensional network containing strong hydrophilic groups, prepared with acrylic acid, methacrylic acid, acrylamide, hydroxypropyl acrylate, and other organic substances through a sol–gel process. The SAP particles were of irregular shape (Fig. 2) with a particle size of 100–1000 μm (Fig. 1 (b)). The bulk density and specific surface area of SAP were 572 kg/m^3 and 14.9 m^2/kg, respectively.

The alkaline activator was prepared by mixing sodium hydroxide, sodium silicate solution, and water at a mass ratio of 0.22:0.8:1. The sodium hydroxide was white flake pellets with a purity of > 96.0 %. The sodium silicate solution with 8.3 wt% Na_2O and 26.5 wt% SiO_2 was a viscous transparent liquid obtained from Shandong Yousuo Chemical Technology Co., Ltd. The initial modulus of the solution was 3.3 and the Bomei degree was 40 °Bé. The final modulus (SiO_2/Na_2O) of the alkali activator was 0.93.

The fineness modulus of standard sand was 2.58. Its apparent density and bulk density were 2630 kg/m^3 and 1460 kg/m^3, respectively. The mixing water was local tap water. The polycarboxylate superplasticizer (PCSP) was provided by Kezhijie New Materials Group. It was a light-yellow liquid with a density of 1.041 g/cm^3.

2.2. Absorption capacity of SAP

Tea-bag method was used to measure the liquid absorption capacity of SAP [20,29]. The SAP was placed in four different solution environments, i.e., deionized water, tap water, simulated pore solution, and AAS supernatant. Among them, the simulated pore solution of proximate components was configured by 0.6 M KOH, 0.2 M NaOH and 0.001 M Ca$(OH)_2$ at a volumetric ratio of 1:1:2 according to Kitowski [40]. The AAS supernatant was obtained by centrifuging the paste for 20 min at a rate of 500 r/min and the suspension was then stilled for 24 h before using.

1 g of dry SAP powder was weighed in a pre-saturated 200 mesh nylon bag and placed in a cup of solution. The use of a pre-saturated bag was to know the influence of absorption by tea-bag method on the obtained sample weight. The container was sealed with a preservative film to prevent water evaporation.

The absorption of SAP at different time points is showed in Fig. 3. It can be seen that SAP showed an increasing absorption with time in all liquids. In deionized water, SAP reached the maximum absorption rate of 26 g/min at 4 min, while the absorption rate of SAP in tap water reached the maximum point of 17 g/min at 8 min. The absorption capacity of SAP in tap water was generally lower than in deionized water due to the presence of ions in tap water. In simulated pore solution and AAS supernatant, the absorptions of SAP were much lower, as consistent to the findings from [29]. After a certain period, the absorption rate of SAP in all solutions began to decrease gradually. At 30 min, the absorption capacities of SAP in the four solutions were 233.9 g/g, 160.7 g/g, 33.2 g/g, and 30.8 g/g, respectively.

The much lower absorption capacity of SAP in simulated pore solution and the supernatant of AAS paste was attributed to the presence of large amounts of ions. On one hand, the anions can compensate the charge of SAP and impair its absorption capacity [41]. On the other hand, the presence of cations especially Ca^{2+} and Al^{3+} can impair the screening effect of the SAP. The repulsive interactions between charged groups within the polymer network are weakened [42] and cross-linking of molecular chains can occur [16], resulting in a significant decrease in the absorption capacity of SAP. This is also in line with the finding of Jenson and Hansen [35].

Fig. 4 shows the water release curve of SAP in drying condition (around 60% relative humidity) after tap water saturation. With the increase of time, the water content of SAP decreased slowly, indicating a

Table 1
Main chemical compositions of slag (wt.%).

Oxide	CaO	Al_2O_3	SiO_2	Fe_2O_3	MgO	TiO_2	Na_2O	SO_3	K_2O	Other	LOI
Slag	47.00	13.01	21.90	0.74	8.07	0.89	0.33	2.50	0.36	2.92	2.28

LOI: Loss on ignition.

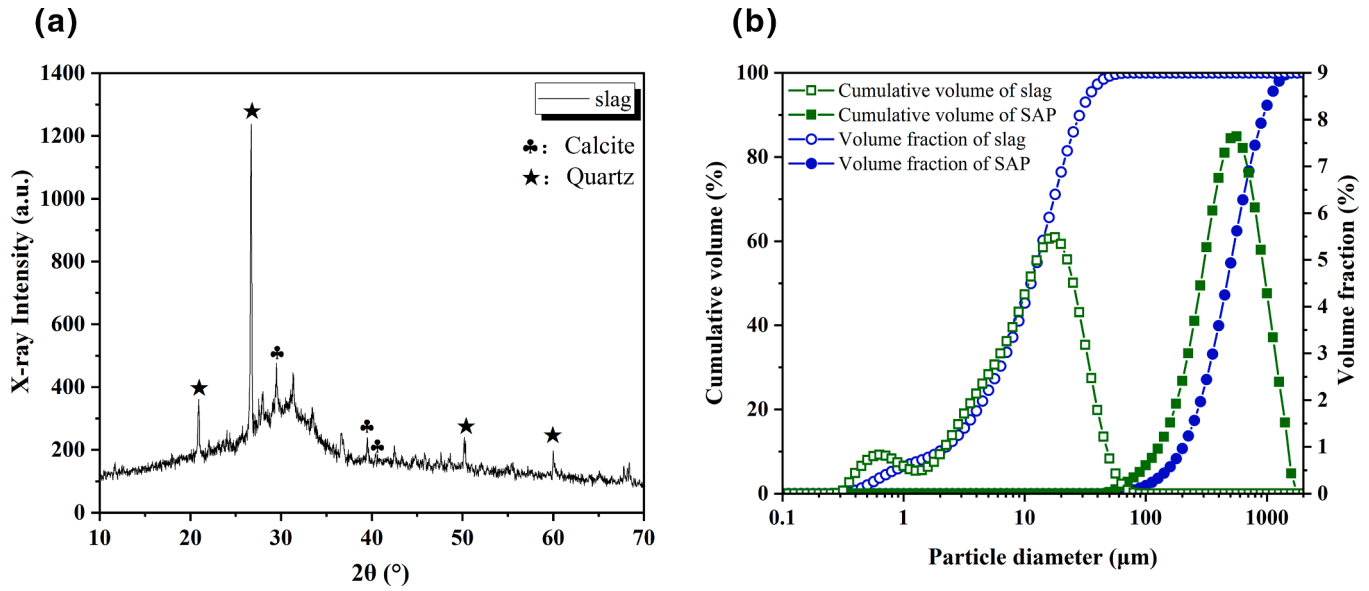

Fig. 1. XRD pattern of the slag (a); Particle size distribution of slag and SAP (b).

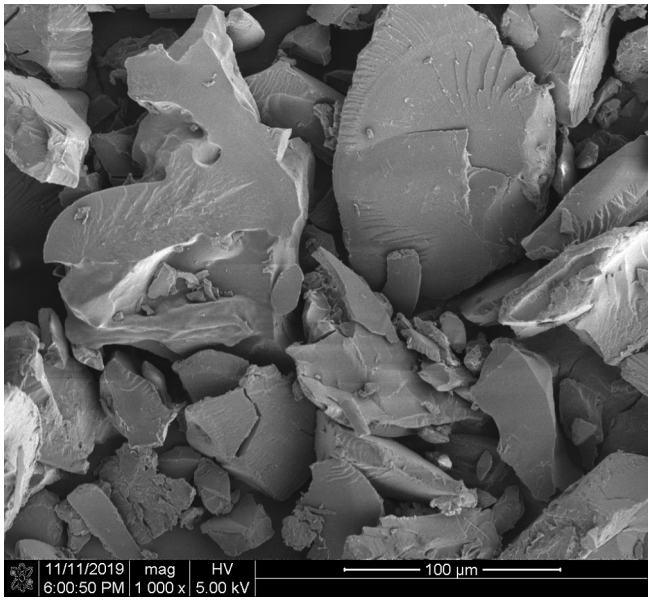

Fig. 2. SEM image of the synthesized SAP particles.

good moisture retention of the SAP. With this capacity, the SAP particles are expected to maintain a high internal relative humidity in the system.

2.3. Mix design

Two ways were used to introduce SAP into AAS mortar.

(1) SAP was mixed with dry powder (D). Firstly, slag and sand were mixed for 1 min. The dry SAP powder was gradually added into slag and sand with the stirring continuing for 1.5 min so that SAP could be uniformly dispersed. Finally, the activator was slowly added to the mixture during stirring. The mixing continued at low speed for 90 s and for another 90 s at high speed.
(2) SAP was mixed with liquid (W). The SAP was first mixed with the activator for 1 min and the suspension was stilled for 10 min before mixed with solids. The time interval of 10 min was chosen based on the following considerations. On one hand, the SAP was allowed to absorb a considerable amount of liquid freely before mixing with solids. On the other hand, the SAP was expected not to be fully saturated before mixing. If the SAP reached its maximum absorption capacity beforehand, no further absorption would be possible during mixing. The presence of more ions in the initial pore solution of the mortar due to the dissolution of slag can cause osmotic pressure and consequently a fast desorption of SAP. In this case, the SAP may soon lose its potential for long-term internal curing. As shown in Fig. 3, the absorption capacity of SAP reached its maximum at 30 min. Hence, 10 min was chosen herein to produce semi-saturated SAP. After that 10 min, the SAP suspension was added into pre-mixed slag and sand. The materials were then mixed for 90 s at low speed and another 90 s at high speed.

The mix proportions of AAS mortar with SAP are shown in Table 2. The liquid-binder ratio was fixed at 0.51 and the binder-sand ratio was 0.56. The activator was sodium silicate solution. The Na_2O content was 4 % by weight of slag. The SAP content gradually increased from 0.05 % to 0.3 % of the mass of slag.

The liquid content was kept constant based on the consideration to set the SAP dosage as the only variable in the mixture components and drying or wet mixing as the only variable in the mixing procedure. As discussed above, the amount of absorbed liquid measured by tea-bag method may not reflect the real absorption of SAP in mortar mixed with different ways. The pre-designed additional liquid-binder ratio would not be accurate and would couple various factors. Hence, the same liquid-binder ratio was used for all mixtures.

2.4. Workability

The workability test was conducted according to ASTM C1437-01 [43] using NDL-3 apparatus. Before casting, wet cotton cloth was used to wipe the disc, the inner wall of the die, the ramming rod and the contact tools with mortar. The mould was put into the center of the table before the fresh mortar was cast in. A tamping bar was used to stamp the mortar for 15 times. After tamping, a small knife was used to remove excess mortar on the surface. Then, the table was immediately vibrated for 25 times at a frequency of once per second. The spread of the mortar after vibration was then measured by a ruler in two perpendicular directions. The average value of the two data was used.

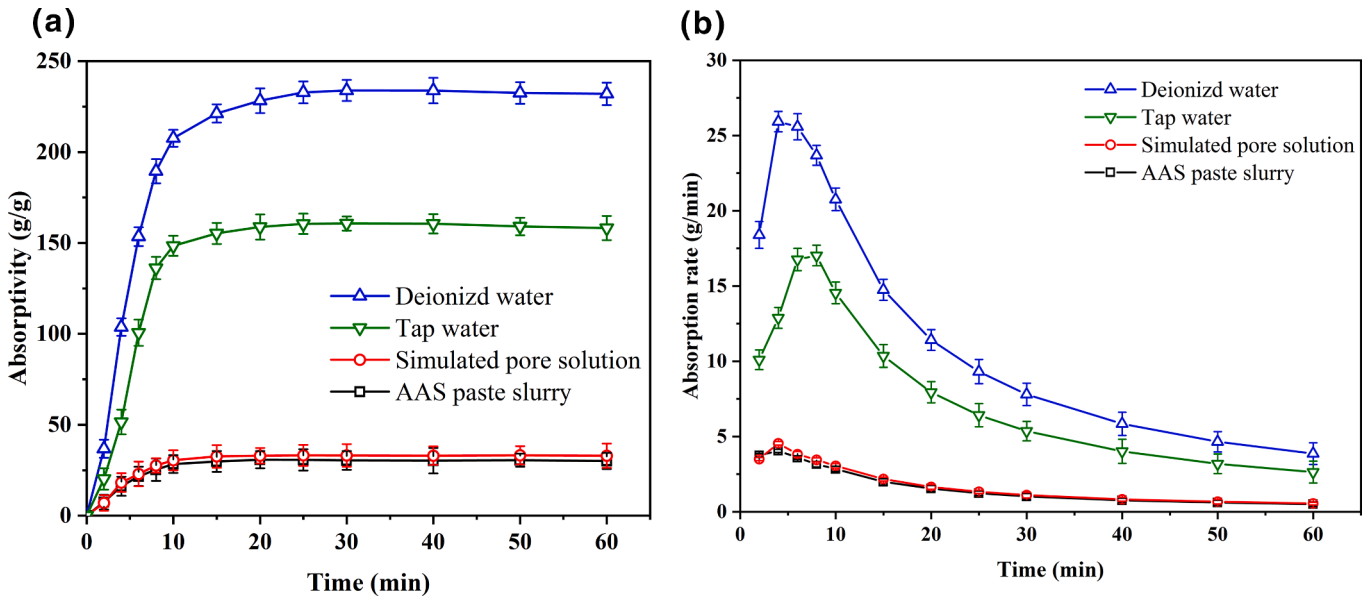

Fig. 3. Absorptivity (a) and absorption rate (b) of SAP in 60 min in deionized water, tap water, simulated pore solution and AAS paste supernatant with the tea-bag method as a function of time.

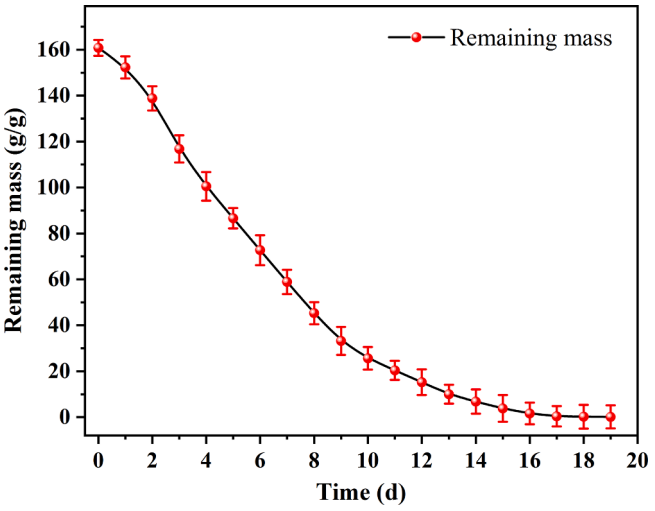

Fig. 4. Remaining mass of SAP in drying condition.

Table 2
Mix proportions of SAP-AAS mortar.

Code	Slag (kg/m^3)	Sand (kg/m^3)	H_2O (kg/m^3)	SiO_2 (kg/m^3)	Na_2O (kg/m^3)	SAP (kg/m^3)	PCSP (kg/m^3)
S0						0	
S0.05D (W)						0.323	
S0.1D (W)						0.646	
S0.15D (W)	646	1292	258.4	35	38.8	0.969	0.646
S0.2D (W)						1.292	
S0.25D (W)						1.615	
S0.3D (W)						1.938	

2.5. Compressive strength

According to Chinese standard GB / T 17671-1999 [44], the compressive strength was measured by a YAW-300C automatic testing machine. The loading rate was 2.4 ± 0.2 kN/s. The samples were cured under 20 ± 2 °C and 98 ± 2 % relative humidity before being tested at the curing ages of 3, 7, 28, and 56 days. At least three specimens were tested in each group, and the average value of strength was obtained.

2.6. Autogenous shrinkage

Referring to ASTM C1698-09 [45], the autogenous shrinkage of AAS paste was measured by a NS-NC-12 shrinkage tester. Paste instead of mortar samples were used for this test aiming at magnifying the difference in shrinkages of different mixtures. The paste mixtures were the same as shown in Table 2, except for the absence of sand. The fresh paste was slowly poured into the corrugated tubes during vibration. The upper plug was tightened gently after filling the tube and the tubes were placed horizontally on the measuring shelf. In order to reduce the friction between the tubes and the shelf, Vaseline was spread around the shelf surface. Three replicates were measured for each mixture. The autogenous shrinkage started from the final setting time of the mixture and the data were recorded every 60 s.

2.7. Permeability

The permeability test was conducted according to Chinese standard JGJ/T 70–2009 [46], using the frustum of a cone sample with a size of 68.5 mm (top) × 80 mm (bottom) × 35 mm (height). After 28 days of curing, the samples were taken out and the surface moisture was removed. Four side surfaces of the cone were sealed by paraffin. The samples were then put into the permeability testing machine and the pressure of water increased from 0 to 0.2 MPa and kept at 0.2 MPa for 2 h. The pressure was increased by 0.1 MPa per hour afterward until 3 out of the 6 samples showed seepage. The final water pressure was recorded and the seepage pressure was calculated according to Eq. (1).

$$P = H - 1 \quad (1)$$

where P is the permeability pressure on AAS mortar, MPa; H is the maximum water pressure on AAS mortar when seepage appears, MPa.

2.8. Frost resistance

According to Chinese standard JGJ/T 70–2009 [46], cube specimens (70.7 mm × 70.7 mm × 70.7 mm) were tested by TR-CLD under multiple freeze–thaw cycles. Three replicates were tested for each mixture. The samples were placed in water at 15 °C ~ 20 °C for 2 d before the curing age reached 28 days. Then the surface water was wiped off and the initial mass of the sample was measured. The test group was put into the freeze–thaw machine, while the control group was put back into the curing room until the freeze–thaw test finished for the test group. The temperature inside the freeze–thaw machine was controlled at −25 °C ~ -20 °C and the freezing lasted for 4 h. Afterward, the samples were taken out and thawed in the water of 15 °C ~ 20 °C for 4 h. 200 freeze–thaw cycles were applied on the samples and the strength loss and mass loss after each cycle were recorded.

2.9. Microstructural characterization

The microstructure of AAS paste with and without SAP was characterized. The mixtures were the same as shown in Table 2 only without sand. The detailed experiments are described below.

2.9.1. Hydration heat

An eight-channel isothermal calorimeter TAM Air was used to measure the early-age reaction heat of the paste. The test temperature was 20 °C and the test last for 1 day. For dry mixing samples, a certain proportion of SAP and slag powder (about 20 g in total) were loaded into the adiabatic sealing bag, and the activator was poured into the adiabatic sealing bag to react. For wet mixing, by contrast, the SAP was first mixed with the activator before being added into slag. About 10 g of the slurry was sucked by a plastic pipette and quickly put into the bottom of the Abe bottle. The bottle was then sealed and immediately put into the test channel of the calorimeter, and the sample containing deionized water was put into another channel as a reference sample.

2.9.2. XRD analysis

XRD analysis was conducted to investigate the crystal compositions of hydration products by X'pert3 powder of Malvern Panalytical with Cu-Kα radiation at 40 kV and 40 mA. The scan step, scan speed, and scope of each sample was 0.02°, 4°/min and 2θ = 5°–80°, respectively. The samples cured for 28 days were crushed into small particles and immersed in isopropanol for a week to stop the reactions. The isopropanol was replaced every 2 days. Then the samples were placed in a vacuum drying chamber at 60 °C until a constant weight was obtained. The AAS paste was ground to particles smaller than 10 μm (through 1600 mesh sieve) before being subjected to the XRD test.

2.9.3. Thermal analysis

STA 449C synchronous thermal analyzer from Niche, Germany was used for thermal analysis of the samples. The samples cured for 28 days were crushed into small particles and the reactions stoppage was stooped. The test environment is helium and the heating rate is 10 °C/min. About 50 mg samples were ground into powders to test for thermal gravimetric analysis.

2.9.4. Scanning electron microscope

For the SEM test, the samples cured for 28 days were broken into small pieces (about 5 mm × 5 mm × 3 mm) by hammer and put into isopropanol for a week to stop the reaction. After drying, the samples were vacuum sealed in the sealing bag until the SEM test. The impurities on the sample surface were removed by tweezers and nitrogen gun. The morphology of the fracture surfaces of the samples was observed by a FEI Quanta 250 tungsten filament scanning electron microscope after gold spraying.

3. Results and discussion

3.1. Workability

Fig. 5 shows the variation in workability of the AAS mortar mixtures. It can be seen that the workability of AAS mortar decreases monotonically with SAP incorporation irrespective of the mixing sequence. The decrease is because the SAP absorbs a certain amount of liquid and reduces the free liquid in the interstitial space between solid particles. However, the decrease in mortars with wet mixing is more significant especially when the SAP dosage is high. This indicates that the SAP particles absorb different amounts of liquid in these two mixing methods. In solution, SAP can absorb liquid freely, therefore the amount of liquid available for mixing with solid becomes lower when more SAP is incorporated, resulting in lower flowability of the mortar. However, when SAP is mixed with solids first, the liquid that it can absorb is limited due to the competition with solids which require a certain amount of liquid to wet and mix. The need for liquid by precursors and sand is not affected by the presence of SAP or not. That is the reason why the flowability of the dry mixed mortar was not much influenced when the SAP dosage was beyond 0.15%.

3.2. Compressive strength

The compressive strength results are shown in Fig. 6. The strength of all mixtures increases with the curing age. Compared to the strength of S0, an improved strength is observed for all SAP-containing mixtures regardless of the SAP dosage and the mixing sequence. This is because the basic liquid-binder ratio is reduced when SAP is present and a denser interstitial structure forms which are beneficial for the compressive strength. By wet mixing, the SAP has chance to absorb more liquid, therefore the strength of wet mixed samples is generally higher than that of the dry mixed ones. Besides, the later release of liquid from SAP (see Fig. 7) will supply extra liquid to the system and contribute to the further reaction of the paste [47]. This point will be verified in Section 3.6.

However, as a liquid reservoir, SAP particles themselves weak points or defects in the matrix. The large pores left in the matrix after SAP release are one of the key ingredients leading to the decrease of compressive strength of AAS mortar [48]. Therefore, the influence of SAP dosage on the strength is not monotonically beneficial. Too much SAP, e.g. 0.3% of slag, results in a lower strength of the mortar than S0.25 with both mixing methods, although the strengths of S0.3D and

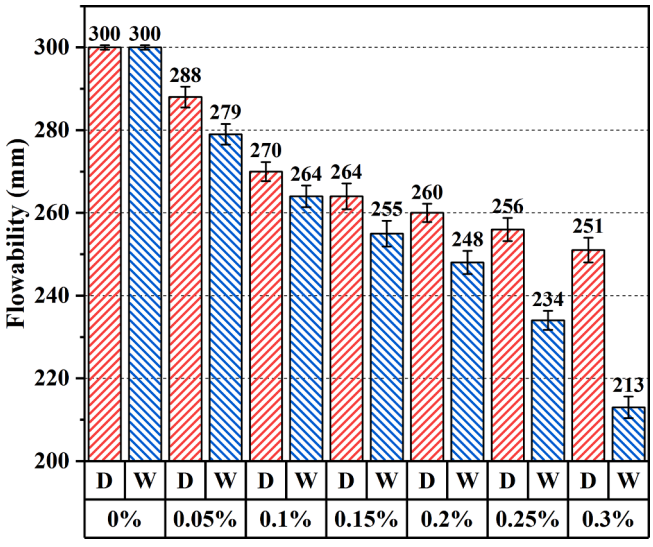

Fig. 5. Flowability of AAS mortar with SAP by dry mixing (D) and wet mixing (W).

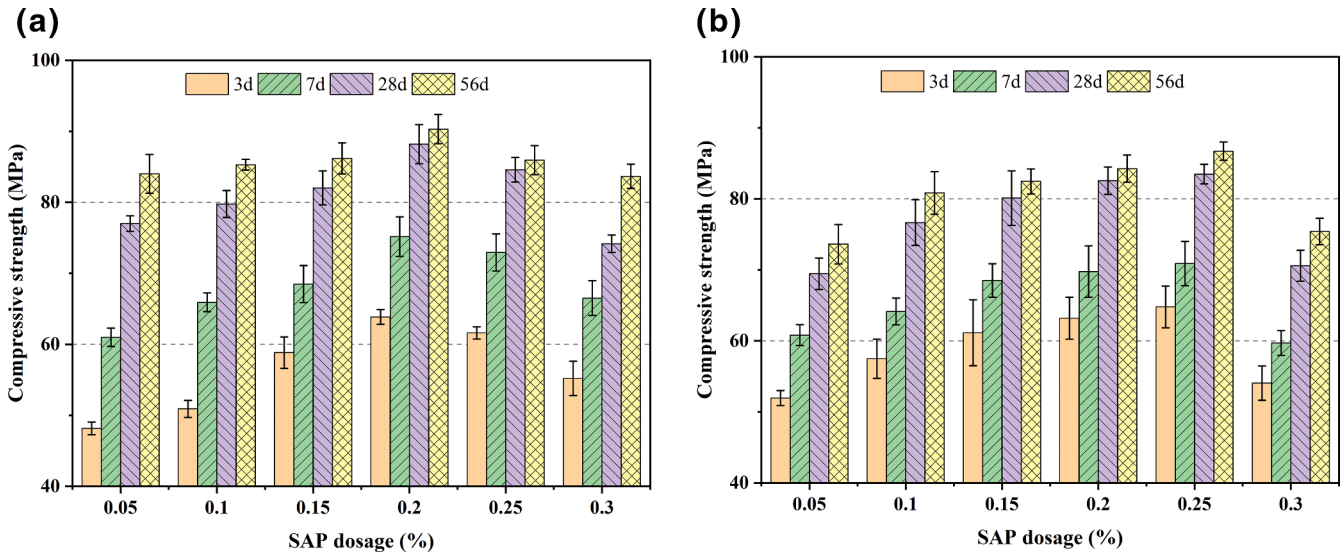

Fig. 6. Compressive strength of AAS mortar with SAP by dry mixing (D) and wet mixing (W).

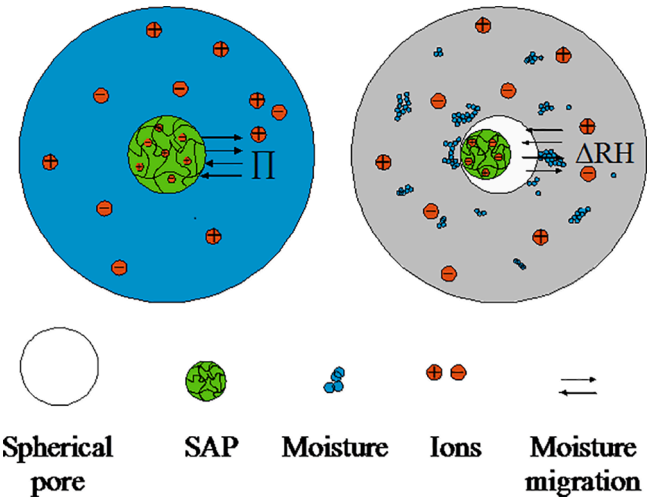

Fig. 7. A schematic image for internal curing of SAP in AAS mortar.

S0.3 W are still higher than that of S0.

3.3. Autogenous shrinkage

A primary purpose of using SAP is to internally cure the matrix to compensate the loss of moisture due to self-desiccation [35]. As a major cause of autogenous shrinkage, self-desiccation occurs along with the formation of reaction products and the densification of pore structures [49,50]. Mitigating the self-desiccation in AAS would be helpful to reduce the autogenous shrinkage and the cracking potential of the restrained concrete [51,52]. Fig. 8 shows the autogenous shrinkage development of AAS pastes with SAP. It can be seen that the major part of the autogenous shrinkage of the pastes develops in the first week and the increase afterwards is not evident. The results in Fig. 8 show that the autogenous shrinkage of AAS paste can be reduced dramatically by SAP. The effect of adding SAP by dry mixing is not as significant as that by wet mixing. This proves that the real absorption capacity of SAP in the dry mixture is relatively lower. With the increase of SAP dosage, the difference induced by different mixing ways becomes less significant. The autogenous shrinkage of S0.2D and S0.2 W is only 48.01 % and 43.09 % of that of S0, respectively. However, it is also noted that however high amount of SAP is incorporated, the autogenous shrinkage of the paste cannot be completely reduced, as consistent with the results reported in [53,54]. This is probably because the self-desiccation is not the only driving force of the autogenous shrinkage of AAS.

The reason why S0.3 W shows higher autogenous shrinkage than S0.3D might be the uneven distribution of SAP in S0.3 W. As discussed above, wet mixing can ensure a larger absorption of liquid by SAP. Nonetheless, a disadvantage of wet mixing is the difficulty to disperse semi-saturated SAP uniformly in the paste. After absorption, SAP particles are stick to each other forming a gel-like stuff and may not be dispersed as homogenously as dry SAP particles in the pastes, especially when the flowability of the paste is rather low (see Fig. 5). Therefore, some part of the paste may not be readily internally cured by the liquid released from the SAP. As a result, the autogenous shrinkage of S0.25 W and S0.3 W is rather similar to that of S0.2 W.

Expansion is observed for all mixtures in the very early age, as shown in Fig. 8 (c) and (d). In general, the expansion magnitude becomes higher and the expansion period becomes longer when more SAP is added inside. It should be noted that the presence of SAP is not the origin of expansion since S0 shows expansion, too. Rather, the expansion is believed to be due to the formation of crystals. In AAS systems, C-S-H (1) (or C-A-S-H) type gel should be the main reaction product in the pastes [55], but there is still possibility of the formation of a small amount of crystals, e.g. hydrotalcite. These hypotheses will be verified in Section 3.6. The total deformation of the system is actually the competition result between expansion and shrinkage. With the reaction going on, the crystals may remain, but the expansion will be gradually compensated by shrinkage. After all, the expansion of all mixtures is below 150 μm/m. The incorporation of SAP reduces the shrinkage in the early age, thus making the expansion more visible in the first hours.

3.4. Permeability

The permeability results are shown in Fig. 9. It can be seen that the incorporation of SAP leads to a lower permeability of AAS mortar. The mechanism behind lies in the modification effect of SAP on the pore structure of the matrix. When SAP is present, a large amount of liquid would be stored in the SAP particles so less liquid would be available in the interstitial space, meaning a lower effective liquid-binder ratio. Unlike the normal capillary pores in the binders, the pores initially occupied by SAP are “ink-bottle” pores, the connectivity of which is much poorer than that of capillary pores. Furthermore, the volume of SAP expands after absorbing water, which can hinder the transport of water in the specimen. Therefore, the SAP-containing mixtures need

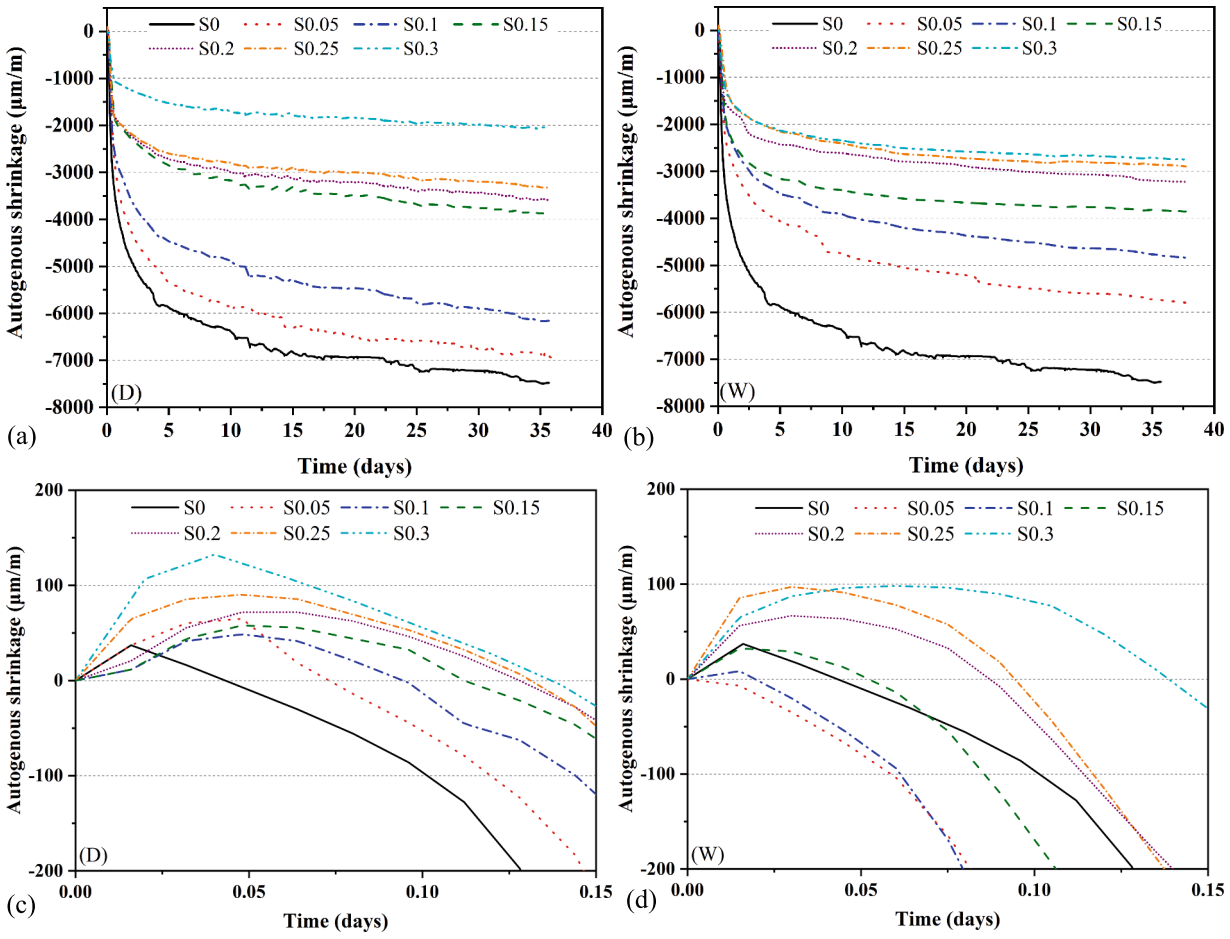

Fig. 8. Autogenous shrinkage of AAS paste with SAP by dry mixing (a) and wet mixing (b). The regions in the very early age are amplified in (c) and (d).

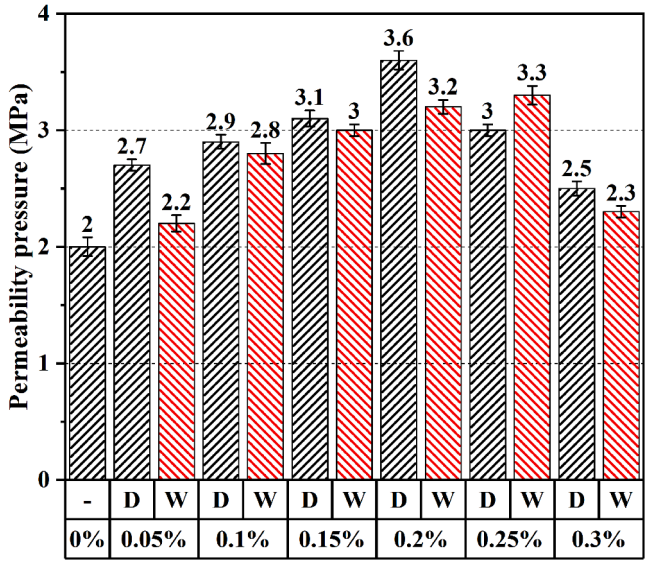

Fig. 9. Permeability of AAS mortar with SAP by dry mixing (D) and wet mixing (W).

higher permeability pressure to be penetrated. However, it is not that the more SAP the better impermeability since too many SAP particles mean too many manually introduced pores and will weaken the matrix. Too much water release will also lead to an increase in porosity, which makes a large quantity of interconnected pores within the specimen accelerate the passage of free water. As shown in Fig. 6, the strength of mortar becomes lower when 0.3% of SAP is added. This effect is more serious for dry mixed samples because a higher amount of SAP than 0.2% in dry mixing cannot absorb much more liquid but introduces more defects into the system. As a result, the impermeability of AAS mortar becomes lower when the SAP dosage is higher than 0.2%. In general, the permeability resistance of dry mixed samples is better than that of wet mixed ones. This might be due to the better distribution of SAP in dry mixed samples, which have less connected pores.

The results in this section indicate that the addition of SAP is beneficial to the impermeability of AAS mortar, but the design is needed in order to identify the optimal SAP dosage.

3.5. *Frost resistance*

The addition SAP was known to be effective in reducing the damage of OPC concrete due to freeze–thaw [56]. The results in Fig. 10 show that SAP has a similar effect in the AAS system. Less severe spalling and lower mass loss are observed for SAP-containing samples as shown in Fig. 10 (a). Consistently, the strength loss of the samples after freeze–thaw cycles is also alleviated by the addition of SAP. Compared with wet-mixed samples, dry mixed ones show slightly better frost resistance, probably due to the more evenly dispersed SAP particles in the matrix. The mechanism behind the improved frost resistance of AAS mortar by SAP is believed to be similar to what has been found for OPC systems. During mixing, SAP absorbs liquid and reduces the free liquid in the capillary pores. After release of liquid, the SAP particles will shrink and leaves space for ice formation due to freezing. With 0.2% of SAP added, the strength loss of AAS mortar is reduced by >40% after 200

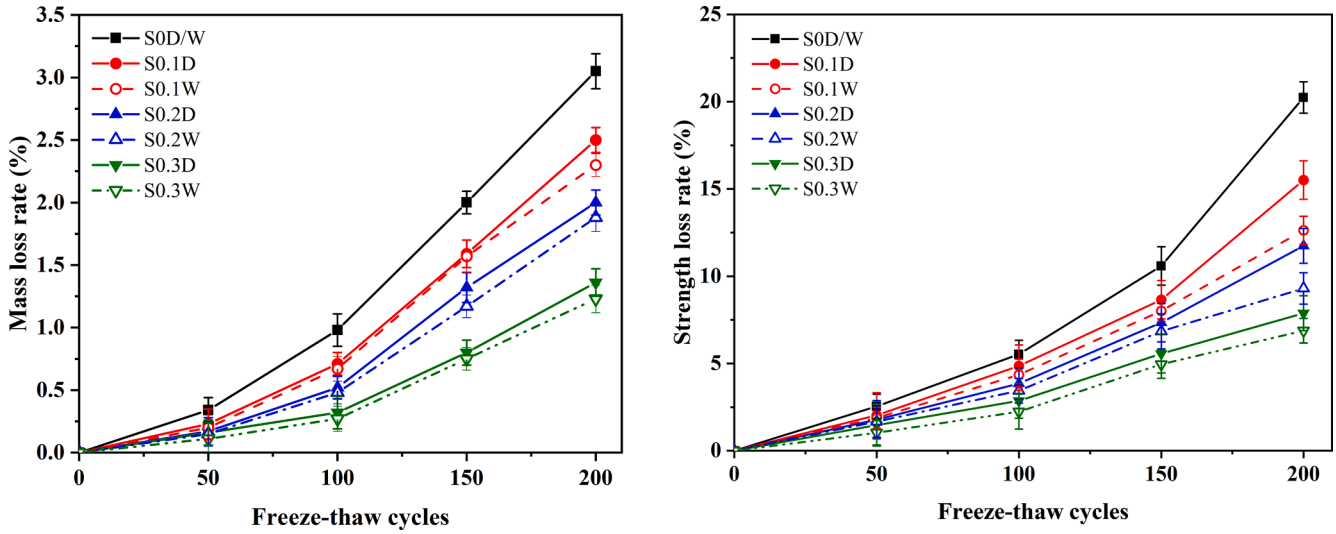

Fig. 10. Freeze-thaw induced mass loss (a) and strength loss (b) of AAS mortar with SAP by dry mixing (D) and wet mixing (W).

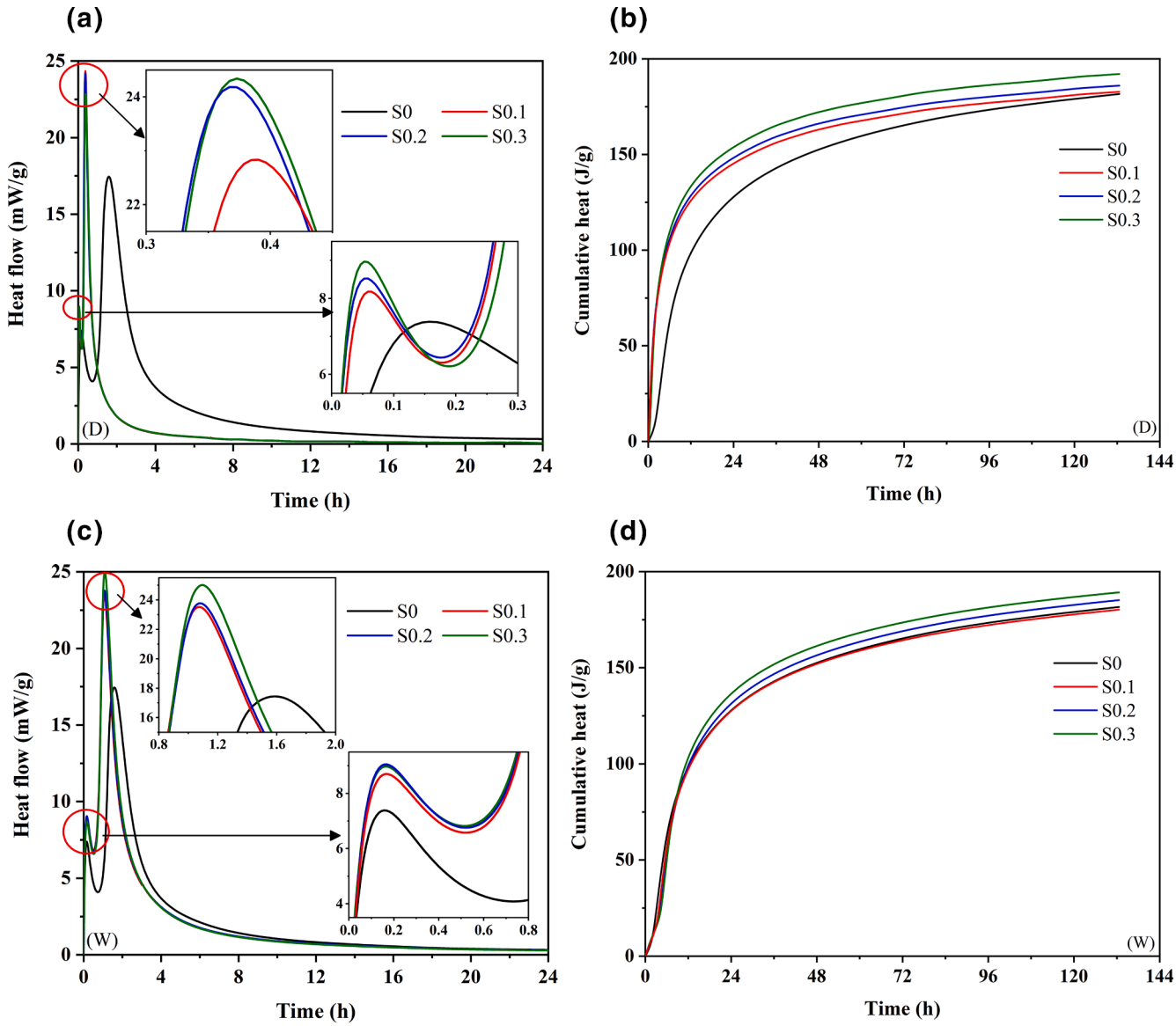

Fig. 11. Reaction heat flow (a and c) and cumulative heat (b and d) of AAS paste with SAP by dry mixing (D) and wet mixing (W).

freeze–thaw cycles.

Summarizing the results in the above sections, it seems 0.2% is the optimal dosage of the SAP which results in a high strength, low shrinkage, and improved durability of AAS mortar. Too little or too much SAP is not beneficial to the overall performance of AAS mortar.

3.6. Microstructural characterization

To explain the abovementioned properties, AAS paste with and without SAP is subject to various characterizations and the results are shown below.

3.6.1. Hydration heat

The heat flow and accumulative heat of the paste mixtures are shown in Fig. 11. Two heat flow peaks are shown by all mixtures. The first peak is normally attributed to the wetting and dissolution of precursors [57]. For dry mixed pastes, the initial heat flow peak occurs earlier when SAP is added probably because the absorption of liquid releases heat. The main reaction peak also occurs earlier. Due to a lower effective liquid-binder ratio of the paste, the concentration of ions dissolved from slag in the pore solution is higher, thus an earlier acceleration period occurs. By wet mixing, the SAP addition also leads to a lower effective liquid-binder ratio, but the release of liquid from SAP can dilute the concentration of ions and buffers the increase of ions concentrations to a threshold level. Therefore, the acceleration period of these samples occurs a bit later than dry mixed samples. Due to the lower initial effective liquid-binder ratio and the later internal curing which can facilitate further reaction, SAP-incorporating mixtures show higher accumulative heat, i.e. higher reaction degree, than the reference mixture, regardless of the mixing way. This point is consistent with the improved strength by SAP as shown in Fig. 6.

3.6.2. XRD analysis

Fig. 12 shows the XRD patterns of AAS pastes under different conditions with various SAP content. It can be seen from Fig. 12 (a) that slag contains a small amount of calcite and quartz, besides the main hump at $2\theta = 25^\circ \sim 35^\circ$. In the patterns for pastes, the peaks of quartz and calcite still exist, but the intensities of the peaks become relatively lower. This shows that the internal curing method is conducive to promoting the hydration and formation of hydrotalcite. When SAP is added, weak diffraction peaks appear in calcite [58]. The presence of a big hump indicates the formation of amorphous products, i.e. C-S-H (1) (or C-A-S-H) gels [55]. Besides that, new diffraction peaks appear at around 12°, which indicates the formation of hydrotalcite as a Mg-Al hydroxide with interlayer-like molecular structure. The formation of hydrotalcite is believed to be the main reason for the expansion shown in Fig. 8. The addition of SAP does not induce the formation of new types of reaction products, only the main hump becomes less sharp. This is probably because the liquid released from SAP facilitates the further hydration of slag, generating not only a higher quantity of products but also products with slightly different compositions from the initial products. The introducing way of SAP seems to have limited influence on the type of reaction products in AAS paste.

3.6.3. Thermal analysis

Fig. 13 shows the TG-DTG curves of AAS pastes. Table 3 shows the mass loss of the samples in each temperature region. In general, the mass loss of the paste becomes higher when more SAP is incorporated. The first mass loss peak at around 100 °C corresponds to the evaporation of physically and chemically bound water from the products, mainly C-S-H (1) (or C-A-S-H) type gels [59,60]. The second peak at around 350 °C is due to the dehydroxylation of the calcium-rich C-S-H (1) (C-A-S-H) type phase [61]. The increased mass loss in these regions with increasing SAP content suggests that the addition of SAP promotes the formation of C-S-H (1) (C-A-S-H) gels, as in line with the results shown in Fig. 11. The small mass loss peak at around 770 °C is mainly attributed to the decarbonization of calcite ($CaCO_3$) to form CaO and CO_2 [62].

The mass loss in wet mixed samples is slightly larger than in dry mixed ones. This proves that SAP absorbs liquid more by wet mixing, which enables better internal curing effect of the SAP.

3.6.4. Scanning electron microscope

The fracture surfaces of two typical mixtures, S0.3D and S0.3 W, are shown in Fig. 14. It can be seen that the matrix of AAS is dense without large capillary pores and the fracture surface is covered by reaction products. The voids left by SAP particles are embedded and dispersed randomly in the matrix. The voids have a non-spherical shape as consistent with the shape of dry SAP particles (Fig. 2). These voids verify that the SAP absorbed a considerable amount of liquid and expanded during mixing. The voids in S0.3 W appear bigger than those in S0.3D, confirming the hypothesis that SAP can absorb more liquid in wet mixing and can provide internal curing afterwards.

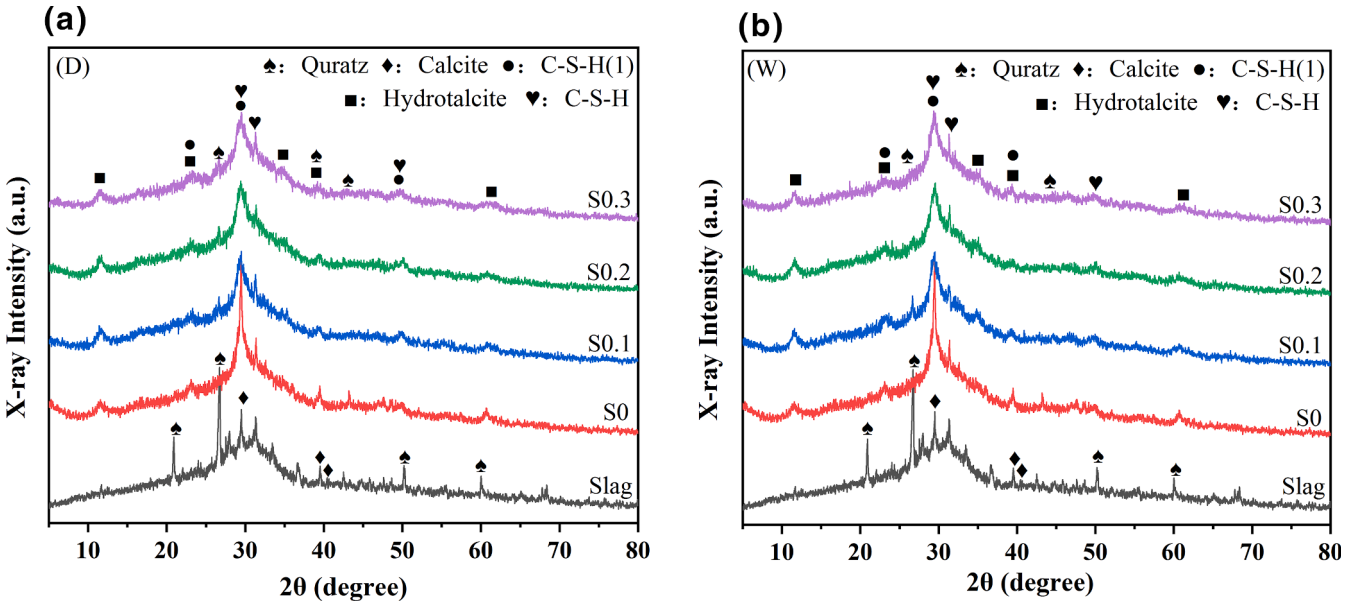

Fig. 12. XRD patterns of AAS pastes with SAP by dry mixing (D) and wet mixing (W).

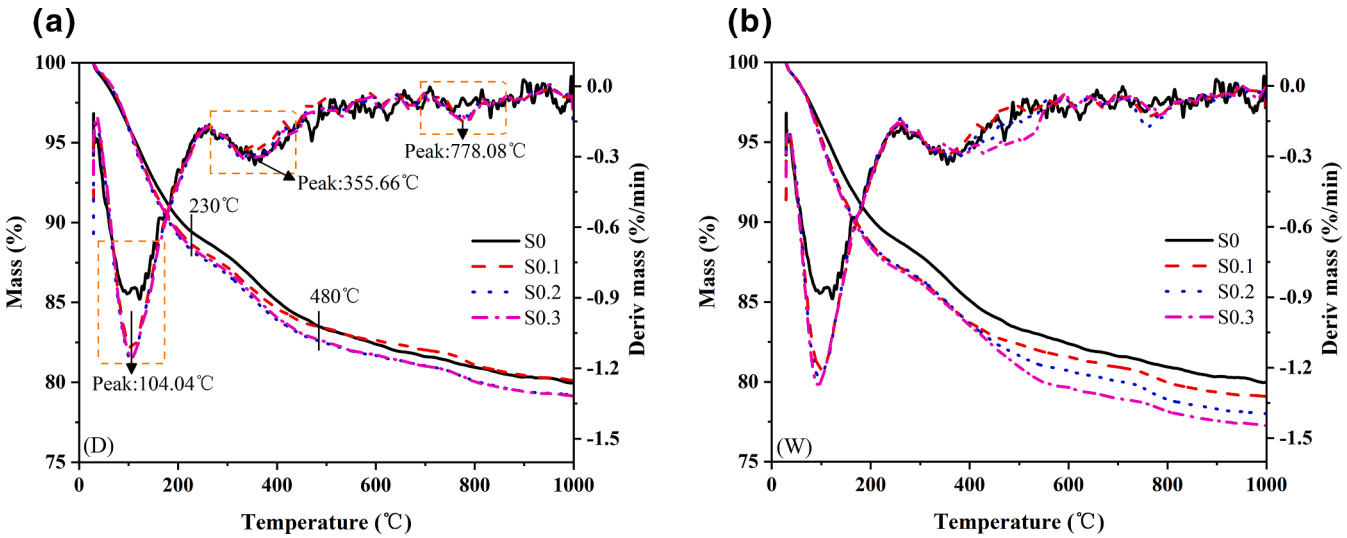

Fig. 13. TG-DTG diagrams of AAS paste with SAP by dry mixing (D) and wet mixing (W).

Table 3
TG mass loss of AAS paste with SAP by dry mixing and wet mixing (%).

Group	Dry mixing			Wet mixing		
	<230℃	230 ~ 480℃	>480℃	<230℃	230 ~ 480℃	>480℃
S0	10.65	5.79	3.60	10.65	5.79	3.60
S0.1	11.43	5.06	3.38	12.26	5.18	3.44
S0.2	11.65	5.52	3.44	12.29	5.79	3.93
S0.3	11.84	5.63	3.57	12.50	6.08	4.16

4. Conclusion

In this paper, the effects of addition of SAP on various properties of AAS systems were investigated. Two mixing methods were used to introduce SAP. The workability, strength, autogenous shrinkage, permeability, and frost resistance of the mixtures were comprehensively studied and explained based on characterization results on the microstructure. The main conclusions of this study are listed below:

1. SAP absorbs the most in deionized water and the least in simulated pore solution and supernatant of AAS. The presence of ions reduces the absorption capacity of SAP.
2. The incorporation of SAP reduces the flowability of AAS mortar when no extra liquid is used. This effect is more remarkable with wet mixing, by which SAP can absorb more liquid.
3. The compressive strength and impermeability of AAS mortar are improved by SAP with a dosage<0.2 % regardless of the introducing way of SAP. The mechanism lies in the lower effective liquid-binder ratio and higher reaction degree of the SAP-containing mixtures.
4. The autogenous shrinkage of AAS paste is mitigated by SAP addition, especially with wet mixing. In the very early age, AAS paste shows slight expansion due to the formation of crystals, and the expansion becomes more intensive when SAP is present.
5. The addition of SAP reduces the damage and strength loss of AAS mortar subjected to freeze–thaw cycles.

The results in this paper suggest SAP is a promising admixture to AAS systems towards a higher strength, lower shrinkage, and better durability. However, design is needed to identify a suitable mixing way and an optimal dosage of SAP.

CRediT authorship contribution statement

Zhengxian Yang: Conceptualization, Methodology, Supervision, Funding acquisition, Project administration, Writing – review & editing. **Peng Shi:** Conceptualization, Methodology, Investigation, Writing –

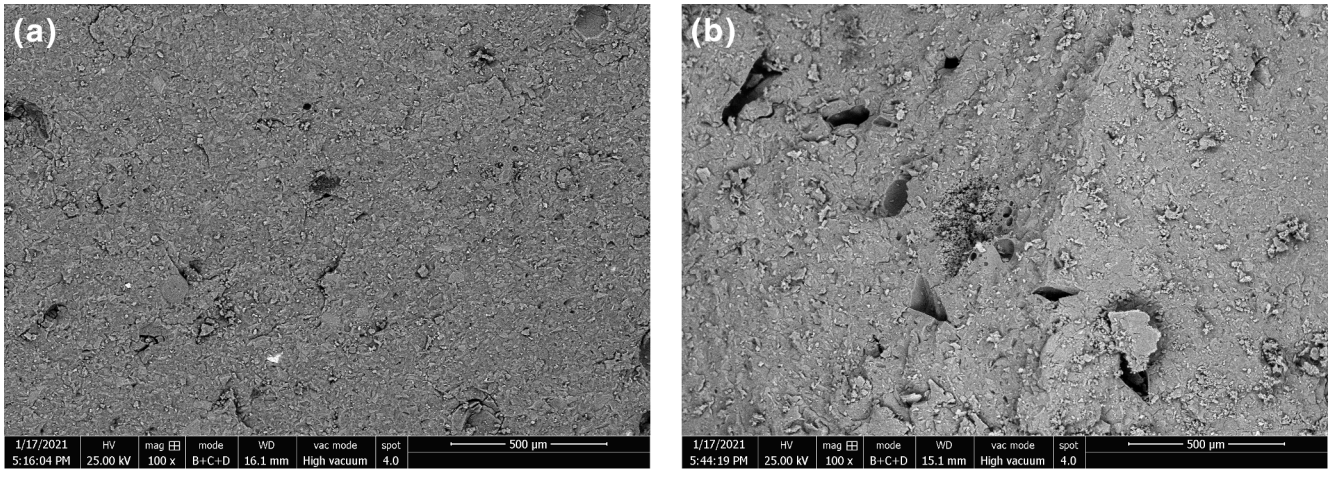

Fig. 14. SEM images of the fracture surfaces of S0.3D (a) and S0.3E (b).

original draft, Writing – review & editing. **Yong Zhang:** Methodology, Investigation. **Zhenming Li:** Methodology, Writing – original draft, Writing – review & editing.

Declaration of competing interest

The authors declare that they have no known competing financial interests or personal relationships that could have appeared to influence the work reported in this paper.

Acknowledgements

This work was financially supported by Minjiang Scholar program of Fujian province, China (GXRC-19045), Natural Science Foundation of China (51978171), Natural Science Foundation of Fujian Province (2019J01235), Fuzhou University Testing Fund of precious apparatus (2020T034), and China Scholarship Council (No.202106650016). The support from Delft University of Technology is gratefully acknowledged.

References

[1] B. Rajini, A.V.N. Rao, Mechanical properties of geopolymer concrete with fly ash and GGBS as source materials, Internat. J. Innov. Res. Sci. Eng. Technol. 3 (9) (2014) 15944–15953.
[2] Z. Shi, C. Shi, J. Zhang, S. Wan, Z. Zhang, Z. Ou, Alkali-silica reaction in waterglass-activated slag mortars incorporating fly ash and metakaolin, Cem. Concr. Res. 108 (2018) 10–19.
[3] A.F. Abdalqader, F. Jin, A. Al-Tabbaa, Development of greener alkali-activated cement: utilisation of sodium carbonate for activating slag and fly ash mixtures, J. Cleaner Prod. 113 (2016) 66–75.
[4] C.J. Shi, A.F. Jiménez, A. Palomo, New cements for the 21st century: The pursuit of an alternative to Portland cement, Cem. Concr. Res. 41 (7) (2011) 750–763.
[5] L. Barcelo, J. Kline, G. Walenta, E. Gartner, Cement and carbon emissions, Mater. Struct. 47 (6) (2014) 1055–1065.
[6] P. Chen, J. Wang, L. Wang, Y. Xu, Perforated cenospheres: A reactive internal curing agent for alkali activated slagmortars, Cem. Concr. Compos. 104 (2019) 103351.
[7] B. Singh, G. Ishwarya, M. Gupta, S.K. Bhattacharyya, Geopolymer concrete: A review of some recent developments, Constr. Build. Mater. 85 (2015) 78–90.
[8] A.R. Brough, A. Atkinson, Sodium silicate-based, alkali-activated slag mortars: Part I. Strength, hydration and microstructure, Cem. Concr. Res. 32 (6) (2002) 865–879.
[9] S.D. Wang, K.L. Scrivener, Hydration products of alkali activated slag cement, Cem. Concr. Res. 25 (3) (1995) 561–571.
[10] M. Nedeljković, Z. Li, G. Ye, Setting, strength, and autogenous shrinkage of alkali-activated fly ash and slag pastes: effect of slag content, Materials 11 (11) (2018) 2121.
[11] Z. Li, B. Delsaute, T. Lu, A. Kostiuchenko, S. Staquet, G. Ye, A comparative study on the mechanical properties, autogenous shrinkage and cracking proneness of alkali-activated concrete and ordinary Portland cement concrete, Constr. Build. Mater. 292 (2021) 123418.
[12] D.B. Kumarappa, S. Peethamparan, M. Ngami, Autogenous shrinkage of alkali activated slag mortars: Basic mechanisms and mitigation methods, Cem. Concr. Res. 109 (2018) 1–9.
[13] T. Lu, Z. Li, H. Huang, Effect of supplementary materials on the autogenous shrinkage of cement paste, Materials 13 (15) (2020) 3367.
[14] B. Zhang, H. Zhu, Y. Cheng, G.F. Huseien, K.W. Shah, Shrinkage mechanisms and shrinkage-mitigating strategies of alkali-activated slag composites: A critical review, Constr. Build. Mater. 318 (2022) 125993.
[15] J. Liu, C. Shi, X. Ma, K.H. Khayat, J. Zhang, D. Wang, An overview on the effect of internal curing on shrinkage of high performance cement-based materials, Constr. Build. Mater. 146 (2017) 702–712.
[16] Z. Yang, P. Shi, Y. Zhang, Z. Li, Influence of liquid-binder ratio on the performance of alkali-activated slag mortar with superabsorbent polymer, J. Build. Eng. 48 (2022) 103934.
[17] S. Oh, Y.C. Choi, Superabsorbent polymers as internal curing agents in alkali activated slag mortars, Constr. Build. Mater. 159 (2018) 1–8.
[18] J. Piérard, V. Pollet, N. Cauberg, Mitigating autogenous shrinkage by internal curing using superabsorbent polymers, in: International RILEM Conference on Volume Changes of Hardening Concrete: Testing and Mitigation, Technical University of Denmark, Lyngby, Denmark, 2006, pp. 20–23.
[19] A. Bentur, S.I. Igarashi, K. Kovler, Prevention of autogenous shrinkage in high-strength concrete by internal curing using wet lightweight aggregates, Cem. Concr. Res. 31 (11) (2001) 1587–1591.
[20] N.K. Lee, S.Y. Abate, H.K. Kim, Use of recycled aggregates as internal curing agent for alkali-activated slag system, Constr. Build. Mater. 159 (2018) 286–296.
[21] J.M. Lin, J.F. Lu, Experimental study on effect for internal curing of porous saturated aggregate on the crack resistance and strength of concrete, Fly Ash Comprehensive Utilization 34 (06) (2020) 68–73, in Chinese.
[22] Mirzabagheri S, Derhamjani G, Maharati S, et al. Using Cuttlebone Powder to Produce Green Concrete. Journal of Applied Engineering Sciences, 2018, 8(21):25-28.
[23] W. Tu, Y.u. Zhu, G. Fang, X. Wang, M. Zhang, Internal curing of alkali-activated fly ash-slag pastes using superabsorbent polymer, Cem. Concr. Res. 116 (2019) 179–190.
[24] M. Wyrzykowski, P. Lura, F. Pesavento, D. Gawin, Modeling of internal curing in maturing mortar, Cem. Concr. Res. 41 (12) (2011) 1349–1356.
[25] V. Mechtcherine, H.W. Reinhardt, Application of Superabsorbent Polymers (SAP) in Concrete Construction: State of the Art Report Prepared By Technical Committee 225-SAP, Springer, Dordrecht Heidelberg London New York, 2012.
[26] F. Wang, J. Yang, S. Hu, X. Li, H. Cheng, Influence of superabsorbent polymers on the surrounding cement paste, Cem. Concr. Res. 81 (2016) 112–121.
[27] C. Song, Y.C. Choi, S. Choi, Effect of internal curing by superabsorbent polymers-Internal relative humidity and autogenous shrinkage of alkali-activated slag mortars, Constr. Build. Mater. 123 (2016) 198–206.
[28] B. Vafaei, K. Farzanian, A. Ghahremaninezhad, The influence of superabsorbent polymer on the properties of alkali-activated slag pastes, Constr. Build. Mater. 236 (2020) 117525.
[29] Z. Li, M. Wyrzykowski, H. Dong, J. Granja, M. Azenha, P. Lura, G. Ye, Internal curing by superabsorbent polymers in alkali-activated slag, Cem. Concr. Res. 135 (2020) 106123.
[30] V. Mechtcherine, E. Secrieru, C. Schröfl, Effect of superabsorbent polymers (SAPs) on rheological properties of fresh cement-based mortars - Development of yield stress and plastic viscosity over time, Cem. Concr. Res. 67 (2015) 52–65.
[31] C. Schroefl, V. Mechtcherine, P. Vontobel, J. Hovind, E. Lehmann, Sorption kinetics of superabsorbent polymers (SAPs) in fresh Portland cement-based pastes visualized and quantified by neutron radiography and correlated to the progress of cement hydration, Cem. Concr. Res. 75 (2015) 1–13.
[32] D. Snoeck, L.F. Velasco, A. Mignon, S. Van Vlierberghe, P. Dubruel, P. Lodewyckx, N. De Belie, The effects of superabsorbent polymers on the microstructure of cementitious materials studied by means of sorption experiments, Cem. Concr. Res. 77 (2015) 26–35.
[33] D. Snoeck, J. Debo, N. De Belie, Translucent self-healing cementitious materials using glass fibers and superabsorbent polymers, Dev. Built Environ. 3 (2020) 100012.
[34] C. Schröfl, V. Mechtcherine, M. Gorges, Relation between the molecular structure and the efficiency of superabsorbent polymers (SAP) as concrete admixture to mitigate autogenous shrinkage, Cem. Concr. Res. 42 (6) (2012) 865–873.
[35] O.M. Jensen, P.F. Hansen, Water-entrained cement-based materials: II. Experimental observations, Cement Concr. Res. 32 (6) (2002) 973–978.
[36] Mehta P K. Concrete: microstructure, properties, and materials. Preticehall International, 2006, 13(4):499-499.
[37] S. Möning, Water saturated super-absorbent polymers used in high strength concrete, Otto Graf J. 16 (2005) 193–202.
[38] Mönnig S, Lura P. Super absorbent polymers (SAP)-An admixture to increase the durability of concrete. Advances in Construction Materials, 2007:351 -35.
[39] M.T. Hasholt, O.M. Jensen, Chloride migration in concrete with superabsorbent polymers, Cem. Concr. Compos. 55 (2015) 290–297.
[40] C.J. Kitowski, H.G. Wheat, Effect of chlorides on reinforcing steel exposed to simulated concrete solutions, Corrosion 53 (3) (1997) 216–226.
[41] S.H. Kang, S.G. Hong, J. Moon, Absorption kinetics of superabsorbent polymers (SAP) in various cement-based solutions, Cem. Concr. Res. 97 (2017) 73–83.
[42] Yao X L. Study on the effect of super absorbent polymer on shrinkage of alkali activated slag cement mortar. Chongqing University, 2017 (in Chinese).
[43] ASTM C1437-01, Standard Test Method for Flow of Hydraulic Cement Mortar, West Conshohocken, PA, 2001.
[44] GB / T 17671-1999, Method of testing cements-Determination of strength. Beijing: China Standard Press, 1999 (in Chinese).
[45] ASTM C1698-09, Standard test methods for autogenous strain of cement paste and mortar, ASTM International, West Conshohocken, PA, 2014.
[46] JGJ/T 70-2009, Standard for test method of basic properties of construction mortar. Beijing: China Construction Industry Press, 2009 (in Chinese).
[47] J. Justs, M. Wyrzykowski, D. Bajare, P. Lura, Internal curing by superabsorbent polymers in ultra-high performance concrete, Cem. Concr. Res. 76 (2015) 82–90.
[48] J. Yang, D. Snoeck, N. De Belie, Z. Sun, Effect of superabsorbent polymers and expansive additives on the shrinkage of alkali-activated slag, Cem. Concr. Compos. 123 (2021) 104218.
[49] O.M. Jensen, P.F. Hansen, Autogenous deformation and RH-change in perspective, Cem. Concr. Res. 31 (12) (2001) 1859–1865.
[50] Q. Huang, X. Zhu, D. Liu, L. Zhao, M. Zhao, Modification of water absorption and pore structure of high-volume fly ash cement pastes by incorporating nanosilica, J. Build. Eng. 33 (2021) 101638.
[51] Z. Li, S. Zhang, X. Liang, G. Ye, Cracking potential of alkali-activated slag and fly ash concrete subjected to restrained autogenous shrinkage, Cem. Concr. Compos. 114 (2020) 103767.
[52] Z. Li, X. Yao, Y. Chen, T. Lu, G. Ye, A low-autogenous-shrinkage alkali-activated slag and fly ash concrete, Appl. Sci. 10 (17) (2020) 6092.
[53] Z. Li, T. Lu, X. Liang, H. Dong, G. Ye, Mechanisms of autogenous shrinkage of alkali-activated slag and fly ash pastes, Cem. Concr. Res. 135 (2020) 106107.
[54] Z. Li, S. Zhang, X. Liang, J. Granja, M. Azenha, G. Ye, Internal curing of alkali-activated slag-fly ash paste with superabsorbent polymers, Constr. Build. Mater. 263 (2020) 120985.
[55] M. Ben Haha, G. Le Saout, F. Winnefeld, B. Lothenbach, Influence of activator type on hydration kinetics, hydrate assemblage and microstructural development of alkali activated blast-furnace slags, Cem. Concr. Res. 41 (3) (2011) 301–310.

[56] V. Mechtcherine, C. Schröfl, M. Wyrzykowski, M. Gorges, P. Lura, D. Cusson, J. Margeson, N. De Belie, D. Snoeck, K. Ichimiya, S.-I. Igarashi, V. Falikman, S. Friedrich, J. Bokern, P. Kara, A. Marciniak, H.-W. Reinhardt, S. Sippel, A. Bettencourt Ribeiro, J. Custódio, G. Ye, H. Dong, J. Weiss, Effect of superabsorbent polymers (SAP) on the freeze-thaw resistance of concrete: results of a RILEM interlaboratory study, Mater. Struct. 50 (1) (2017).
[57] A.R. Sakulich, D.P. Bentz, Mitigation of autogenous shrinkage in alkali activated slag mortars by internal curing, Mater. Struct. 46 (8) (2013) 1355–1367.
[58] W. Zheng, J. He, Y. Tong, J. He, X. Song, G. Sang, Investigation of effects of reactive MgO on autogenous and drying shrinkage of near-neutral salt activated slag cement, Ceram. Int. 48 (4) (2022) 5518–5526.
[59] T. Yang, H. Zhu, Z. Zhang, X. Gao, C. Zhang, Q. Wu, Effect of fly ash microsphere on the rheology and microstructure of alkali-activated fly ash/slag pastes, Cem. Concr. Res. 109 (2018) 198–207.
[60] X. Zhu, M. Zhang, K. Yang, L. Yu, C. Yang, Setting behaviours and early-age microstructures of alkali-activated ground granulated blast furnace slag (GGBS) from different regions in China, Cem. Concr. Compos. 114 (2020) 103782.
[61] Danielson U H. Heat of hydration of cement as affected by water-cement ratio. Proceedings of the 4th international Symposium on the Chemistry of Cement, Washington DC, U. S., Paper Ⅳ-S7, 1962:519-526.
[62] B.S. Gebregziabiher, R. Thomas, S. Peethamparan, Very early-age reaction kinetics and microstructural development in alkali-activated slag, Cem. Concr. Compos. 55 (2015) 91–102.